Ansari, R. I., Pervaiz, H., Hassan, S. A., Chrysostomou, C., Imran, M. A., Mumtaz, S. and Tafazolli, R. (2019) A new dimension to spectrum management in IoT empowered 5G networks. IEEE Network, 33(4), pp. 186-193.

http://eprints.gla.ac.uk/181764/

Deposited on: 13 March 2019

A New Dimension to Spectrum Management in IoT Empowered 5G Networks

Rafay Iqbal Ansari, Haris Pervaiz, Syed Ali Hassan, Chrysostomos Chrysostomou, Muhammad Ali Imran, Shahid Mumtaz and Rahim Tafazolli

Abstract—**Paving the way for future 5G technologies requires a need to overcome the spectrum crunch, which is one of the major challenges impeding the growth of wireless technology. The issue at hand becomes more pronounced when we consider Internet-of-Things (IoT), where billions of devices require connectivity. This article motivates the need for exploring new spectrum opportunities with reference to the requirements of IoT networks. Millimeter wave (mmWave) spectrum is considered as a panacea for overcoming the spectrum crunch, providing the much needed breathing space for introducing new applications that require higher rates. A network based on control/data separation architecture (CDSA) could further improve the performance by utilizing the mmWave-based data base stations (DBSs). The control base station (CBS) operates on the sub-6 GHz single band, while the DBS possesses a dual-band capability. This article presents a new dimension to spectrum heterogeneity by utilizing a dual-band approach at the DBS. One of the unique aspects of this work includes the analysis of a joint radio resource allocation algorithm based on Lagrangian Dual Decomposition (LDD) and we compare the proposed algorithm with the maximal-rate (maxRx), Dynamic sub-carrier allocation (DSA) and Joint power and rate adaptation (JPRA) algorithms. The analysis is further expanded by showing an interplay between the utilization of licensed and unlicensed mmWave resources and how the dynamic spectrum management could help in their efficient utilization.**

I. INTRODUCTION

Future 5G networks hold great prospects for introducing new applications that provide users with a unique quality of experience (QoE). The interconnection between a high number of devices in the so called Internet-of-Things (IoT) networks, signifies the need for higher capacity to support the desired QoE. In order to meet the ever increasing demands for capacity, a new air interface known as 5G New Radio (5G NR) has been introduced. The first stage of development of 5G NR is based on the improvements in microwave-based (μW) long term evolution (LTE) and long term evolution-advanced (LTE-A). However, the emergence of new and innovative applications with enhanced QoE demands have rendered the conventional μW networks insufficient and have signified the

need for exploring other spectrum opportunities. The aim of this article is to identify the prospects and challenges with regards to the new opportunities.

During the previous decade, the concept of heterogeneous networks (HetNets) has gained ground as both academia and industry consider HetNets as a prime technology that could alleviate the situation with regards to spectrum management. HetNets are based on the concept of multi-tier networks with macrocells overlaid with small cells (micro, pico and femto). The concept behind the introduction of small cells is to reduce the distance between access network and the users, thereby improving the link quality. The traffic from macrocells is offloaded to small cells, relieving the burden on macrocells and allowing more and more users to gain access to high quality links provided by small cells. Small cells based on Millimeter wave (mmWave) frequency band (30 GHz to 300GHz) are considered as a potential candidate for providing the much needed space with regards to new spectrum opportunities and to avoid spectrum congestion. In the subsequent sub-sections, we overview the inevitable components of future networks, i.e., massive deployment of devices, the concept of green communications, and radio resource management in these networks, and then blend them together in the rest of the article to present an efficient system model.

A. Massive Internet-of-Things

One of the main objectives of 5G networks is to support applications that involve a high density of devices. In this regard, the concepts of massive machine-type communications (mMTC), enhanced mobile broadband (eMBB) and ultra-reliable low-latency communications (URLLC) are being developed to support such applications. Machine-to-machine (M2M) is a concept associated with the future IoT, where billions of devices would be connected to the internet. The growth in industrial IoT has further aggravated the situation, where the applications based on the IoT platform are related to health, agriculture, automobile, power and environment sector, among others [1]. The requirement of providing ubiquitous connectivity to the massive IoT (mIoT) devices highlights the need for exploring new spectrum opportunities. The IoT traffic will increase as we move towards realizing applications with high rate requirements, lending credence to the need for overcoming the spectrum scarcity. However, energy efficiency is one of the key challenges with regards to mIoT. In the sequel, we highlight the need for energy efficient solution and the associated tradeoffs.

R. I. Ansari and C. Chrysostomou are with the Department of Computer Science and Engineering, Frederick University, Nicosia, Cyprus. Emails: rafay.ansari@stud.frederick.ac.cy, ch.chrysostomou@frederick.ac.cy.

H. Pervaiz (**Corresponding Author**) and R. Tafazolli are with Institute of Communication Systems, Home of 5GIC, University of Surrey, UK. Emails: {h.pervaiz, r.tafazolli}@surrey.ac.uk.

S. A. Hassan is with the School of Electrical Engineering & Computer Science (SEECS), National University of Sciences and Technology (NUST), Pakistan. E-mail: ali.hassan@seecs.edu.pk.

M. Imran is with the School of Engineering, University of Glasgow, UK. Email: Muhammad.Imran@glasgow.ac.uk.

S. Mumtaz is with the Instituto de Telecommuninic̨oes, DETI, Universidade de Aveiro, Aveiro, Portugal. Email: smumtaz@av.it.pt.

B. Green Communication Networks

The concept of green communications is emerging, where several new techniques have been introduced to enhance the energy efficiency (EE) of a network. Wireless networks comprise of energy hungry base stations (BSs), which highlights the need for ensuring EE with regards to the BS operation. Moreover, the energy consumption becomes more pronounced when we consider massive deployment of devices. Energy consumption can be reduced by employing dynamic resource allocation techniques that ensure optimal utilization of resources. However, it is important to identify the performance tradeoffs with regards to the EE, i.e., maximizing the EE can have detrimental impacts on other performance metrics such as outage probability [2] [3]. Moreover, the energy consumption of a wireless network also depends on the desired quality-of-service (QoS), e.g., a higher transmission success may lead to higher energy consumption. Therefore, in this article, we motivate the need for dynamic radio resource allocation that maximizes the spectral efficiency (SE) and EE of the network.

C. Radio Resource Management

Dynamic spectrum management techniques allow the devices to switch between different options, thereby increasing the overall network capacity by providing more degrees of freedom [4]. The resource management problem becomes more pronounced when ultra dense network (UDN) deployment based on mmWave technology is considered. In the context of UDNs, the network performance gains such as EE can only be enhanced by developing network optimization framework. A dynamic user association and power allocation mechanism allows the optimal utilization of resources, while keeping in view the network constraints [5]. Recently, the concept of dual-band BSs has been explored for mitigating the interference and providing higher transmission bandwidths. Utilizing two different frequency bands with different propagation characteristics could provide significant performance gains in terms of network capacity [6]. A dual-band approach may involve utilization of sub-6 GHz and mmWave band. In such a network, the user is able to associate with low data rate but more reliable sub-6 GHz links or high data rate but relatively unreliable mmWave links [7]. This integrated mmWave/sub-6 GHz approach allows shared use of unlicensed and licensed spectrum and highlights the need for dynamic radio resource management.

D. Contributions of this work

In this work, we utilize the concept of control data separation architecture (CDSA), where the main concept behind CDSA is to separate the control plane (CP) and the data plane (DP). The CP operates at lower frequencies so that larger coverage could be ensured. On the other hand, DP can operate on higher frequency bands such as the mmWave bands for providing higher capacity and more spectrum opportunities. The nomenclature of CDSA architecture includes control BSs (CBSs) that correspond to the macrocells, while the data
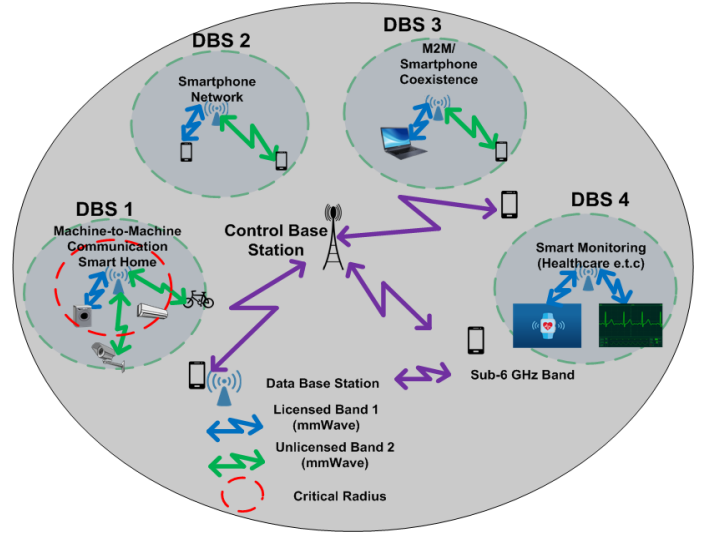

Figure 1: System model: Integration of licensed/unlicensed band based on CDSA

BSs (DBSs) correspond to the small cells, which overlay the CBSs. A detailed discussion on the CDSA architecture and its potential benefits is presented in Section II.

In view of the challenges posed by future dense networks, in this article, we present a system model that employs the concept of CDSA and motivates a new dimension to spectrum heterogeneity by analyzing a dual-band approach based on using both licensed and unlicensed spectrum. We employ a dual-band approach at the DBS, where the DBS operates in both unlicensed 26 GHz and licensed 60 GHz mmWave frequency band. Viewing the importance of ensuring an energy-efficient solution, we develop a multi-objective optimization problem, which jointly optimizes conflicting objectives to analyze the SE and EE. One of the unique aspects of this work includes the analysis of a joint radio resource allocation algorithm based on Lagrangian Dual Decomposition (LDD). The LDD-based algorithm jointly optimizes the decisions with regards to power allocation for CBS and DBS, conducts sub-carrier pair allocation and determines the choice of transmission strategy. Towards the end of the article, we present a case study that provides a designer's perspective for a network based on CDSA, complemented by a dual-band approach. We also present a comparison of relevant power allocation schemes with our proposed scheme by quantifying the achievable EE and SE.

II. CONTROL-DATA SEPARATION ARCHITECTURE

The 4G cellular networks prohibit to cater the future demands, which highlights the need for exploring new opportunities. CDSA has been introduced as a key technology for realizing new applications. The CDSA can prove beneficial in UDNs, with the dense deployment of mmWave DBSs to provide better SE by the efficient utilisation of radio resources, whereas the controlling and signaling can be efficiently provided by the CBS [8].

The CDSA promises to overcome the limitations of traditional networks by providing ubiquitous coverage and is well

suited for diverse applications and use cases defined for the 5G networks. Moreover, the CDSA allows to distinguish between active and idle modes of the cellular users (or IoT devices), which helps in efficient allocation of resources. The active devices[1] establish association with both the CBS and DBS, while the idle devices are only connected to the CBS. When a device initiates any activity, the CBS can designate the best DBS to the device. The DBSs can be densely deployed in UDNs, but they can be switched off during the low/off peak traffic loads in order to reduce the energy consumption.

In contrast to the conventional cellular networks, CDSA manages the issue of frequent handovers by utilizing a mobility management mechanism that incurs lower signaling overhead [8]. The handovers taking place between DBSs falling within the coverage area of CBS are centrally managed, leading to lower signaling overhead and smooth handovers. Fig. 1 depicts the deployment of CBSs and DBSs for empowering IoT applications, where each DBS possesses a dual-band capability to provide transmission to its devices and CBS operate on a single sub-6 GHz band. In the subsequent section, we build the case for combining the dual-band network operation with CDSA and discuss the importance of a radio resource management technique for optimal performance of dual-band mmWave with CDSA.

III. CASE STUDY: A NEW DIMENSION TO SPECTRUM HETEROGENEITY

Deviating from traditional spectrum heterogeneity involving integration of sub-6 GHz band with the mmWave bands, we, herein, employ a dual-band approach at the DBSs, where each DBS operates at both licensed and unlicensed mmWave frequency bands. Our aim is to extend the CDSA architecture to investigate the dual band mmWave DBSs as a possible solution to develop a joint energy and spectral efficient radio resource management procedure to provide energy savings in comparison to the traditional networks. The studies reveal that the power consumed in the BS comprises of 80% of the total energy consumption of the network. The high share of power consumption by the BS highlights the need for ascertaining an energy-efficient solution for the ultra-dense networks [9]. The CDSA architecture can be further categorized into the following cases as listed below:

1) The CBS is responsible for supporting the CP only, while the DP is supported by the DBS.
2) The CBS is responsible for supporting both the CP as well as the DP, while the DBS supports the DP.

The average traffic load at different time intervals of the day at each DBS can be predicted by self-learning traffic prediction mechanisms based on the historical call data records using support vector machine (SVM) regression model. The historical data is split into the training and testing datasets. The traffic prediction module is trained on the training dataset and then it predicts the average traffic load for the considered DBS for the testing dataset to evaluate the accuracy and precision of the proposed training prediction mechanism. In our model,

---

[1] The term devices refer to both cellular users or IoT devices

the whole day is divided into 24 equal time intervals with duration of one hour, where the time intervals are denoted by $t \in \{t_1, t_2, \cdots t_{24}\}$. It is also assumed that the average traffic load remains constant within the two measuring time intervals, however, the devices are assumed to be moving with the speed of 3 km/hr randomly within the coverage area of the DBS and the CBS.

Fig.2 depicts the proposed CDSA architecture with licensed and unlicensed mmWave bands DBSs f_2 and f_3, respectively, by employing the realistic blockage model overlaid within the geographical coverage region of the single band CBS on f_1. Once the average traffic load for each DBS at the time interval t_i is predicted, $i = \{1, 2, \cdots 24\}$, the devices are associated with either CBS or DBS along with the selection of the frequency bands, $f \in \{f_1, f_2, f_3\}$, which is followed by the resource block (RB) allocation. The partitioning of radio resources among the CBS and DBS for both signaling/controlling and data transmissions are quite dependent on the factors such as density of devices, density of DBSs, the propagation environment including areas covered by the buildings, height distribution of the buildings and the locations/heights of the DBSs that impact the blockage model.

In this trend, this work investigates the impact of the partition of spectral resources among the CBS and DBSs on the system performance such as achievable EE and SE. It is assumed that there are N_1 RBs exclusively reserved for the CBS operating at f_1 band based on its operating bandwidth, whereas the total number of RBs at DBSs operating at f_2 and f_3 bands are assumed to be N_2 and N_3, respectively. The total number of RBs at the CBS can be divided into two orthogonal sub-partitions, namely as N_{DBS}^C and $\overline{N_1}$. N_{DBS}^C is the set of RBs reserved exclusively for the unserved devices covered by the DBSs while initiating the data connections with the CBS. $\overline{N_1}$ can be further repartitioned into N_{CBS}^D and N_{CBS}^C, respectively, where N_{CBS}^D is the set of RBs that serve the devices that are provided data coverage by the CBS. N_{CBS}^C is the set of RBs reserved for the control and signaling mechanisms of the CBS. For the simplicity of the analysis, we define the proportion of the RBs reserved by the CBS (or ratio of N_{DBS}^C and N_1) for providing data transmission to the unserved devices lying within the DBS by α. Similarly, the proportion of the RBs reserved by the CBS (or ratio of N_{CBS}^D and $\overline{N_1}$) for providing data transmission to the unserved devices lying within the CBS by β.

One of the key contributions of this work is to provide some design insights to the network providers to dynamically adjust the partition of resources among the CBS and DBS considering the aforementioned factors of the simulated environment and the priority of the two considered objectives (EE and SE) to obtain the better system performance. In this regard, the joint EE and SE maximization problem is formulated as a multi-objective optimization (MOO) problem, which tries to maximize the two conflicting objectives simultaneously subject to the partition of spectral resources among the CBS and DBSs, the minimum QoS requirements, and maximum input power constraint. The MOO problem is transformed into a single objective optimization (SOO) problem using the Weighted Tchebycheff method [10]. The transformed SOO problem can
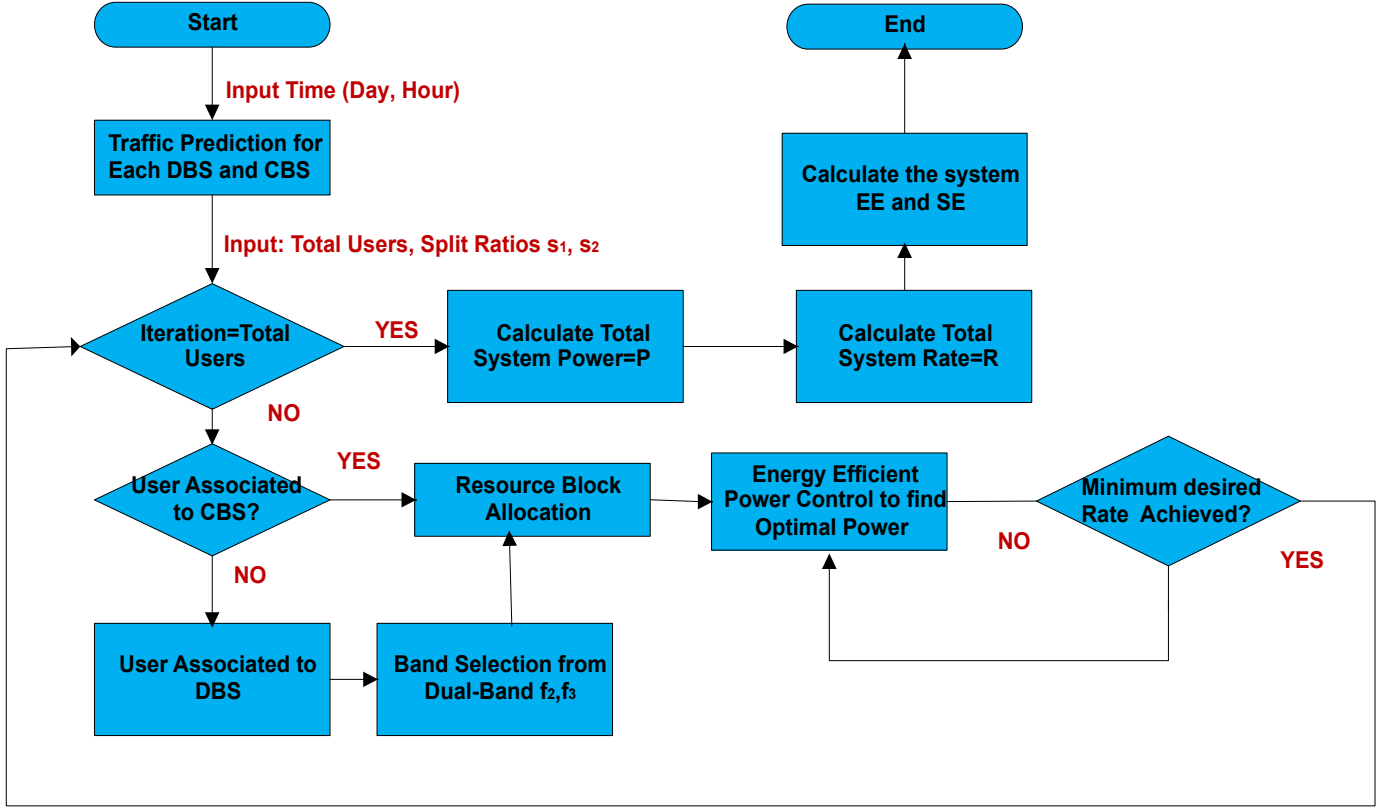
Figure 2: Proposed radio resource management procedure CDSA-based 5G networks

be solved using standard interior point methods, such as LDD method, allowing us to obtain the Pareto optimal solution resulting in a complete Pareto-Frontier curve by dynamically adjusting the weights of both the objectives. The main steps outlined in the proposed radio resource management procedure to evaluate the system performance in terms of the achievable SE and EE are depicted in Fig. 2. We have defined EE as the ratio of total system power and total system rate observed at per unit bandwidth, while the SE is defined as the ratio of total system rate and system bandwidth.

A. Simulation Setup and Performance Evaluation

In this article, our emphasis is on the *Case 2*, where the CBS is responsible for supporting both the CP as well as the DP, while the DBS supports the DP. We analyze the proposed CDSA network consisting of dual band DBSs lying within the coverage region of a single band CBS in the downlink transmission scheme as depicted in Fig. 1, assuming that perfect channel state information (CSI) is available at the CBS. We assume that the sector level beam alignment is already established and the coarse grained beam level alignment takes place in order to establish the high directivity links. We further assume that the CBS is operating at the unlicensed sub-6 GHz industrial, scientific and medical (ISM) band, namely as f_1 = 2.4 GHz with an operating bandwidth of 20 MHz, resulting in N_1 = 100 RBs. The DBSs are operating at the licensed mmWave band, f_2 = 26 GHz and unlicensed mmWave band, f_3 = 60 GHz with an operating bandwidth of 1

GHz, and we assume the total number of RBs as N_2 = 192 and N_3 = 192 in each band, respectively. In this work, we don't strictly follow the 5G new radio (5G NR) recommendations regarding variable RB size. Moreover, we assume that the RB size N_1, N_2 and N_3 is fixed and it doesn't vary with the traffic requirements. However, our system model is flexible and can be analyzed for different values of frequencies and RBs. In the simulation environment, we assume 6 DBSs lying within the geographical coverage region of the CBS with randomly distributed devices within the region of interest. The maximum transmission ranges of the CBS and the DBSs are assumed to be 1 km and 100 m, respectively. A maximum of 10 devices are assumed within the coverage area of a DBS. Moreover, the number of devices outside the coverage area of DBSs and distributed within the coverage area of CBS is also assumed to be 10.

The links operating at the sub-6 GHz band follow Rayleigh small scale fading, whereas Nakagami fading is assumed for the links operating at mmWave bands. The noise spectral density is assumed to be -174 dBm/Hz. The blockage model considered in this analysis is a rectangle Boolean scheme giving the probability of the line-of-sight (LoS) link as the negative exponential function of the distance d between the devices and the DBS, e.g., $\exp\{-\mu d\}$. It is important to highlight that μ is dependent on the size and density of the blockages [11]. We apply this LoS probability function based on the real building statistics of the simulated envi-ronment [11]. There is a simplified version of the Boolean
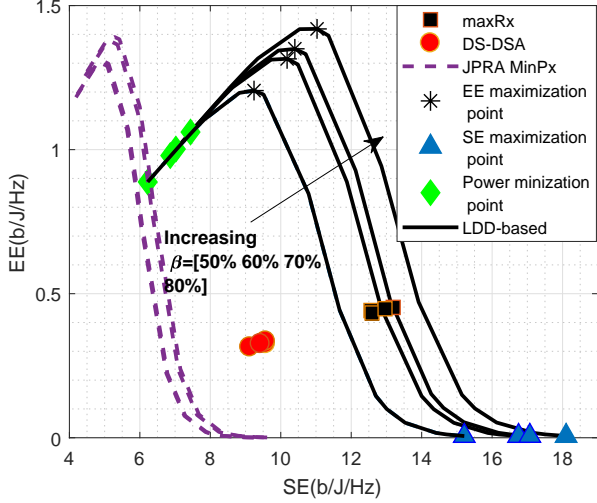
Figure 3: Energy-efficiency versus spectral-efficiency with $\alpha = 50\%$ and $\beta = [50\% \ 60\% \ 70\% \ 80\%]$ at the measuring time interval t_5, average traffic load $L_{\text{DBS}} = [50\% \ 30\% \ 30\% \ 60\% \ 20\% \ 30\%]$
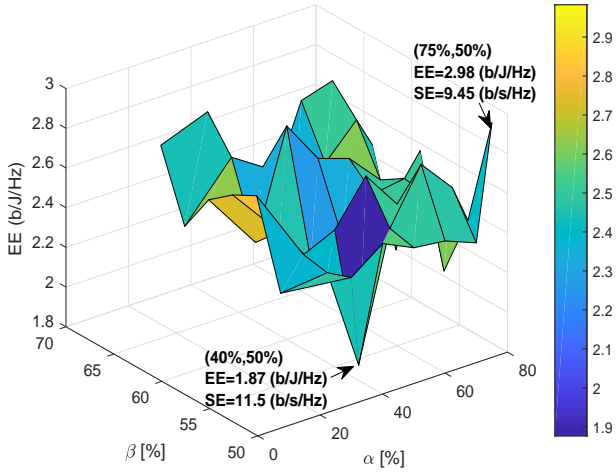

Figure 4: Energy-efficiency variation with different sets of α and β at the measuring time interval t_{10}, average traffic load $L_{\text{DBS}} = [40\% \ 25\% \ 30\% \ 45\% \ 50\% \ 35\%]$

rectangular scheme wherein the link between the devices and the DBS is assumed LoS if it falls within the critical radius R_C, and non-line-of-sight (NLoS) otherwise [12].

The path loss exponent for NLoS and LoS links are assumed to be $\rho_n = 4$ and $\rho_l = 2$, respectively whereas the path loss exponent for transmissions at sub-6 GHz band is assumed to be 2.7. The standard deviation of shadowing for NLoS and LoS links are assumed to be 7.2 dB and 5.2 dB, respectively. The sector level beamwidth is assumed to be 90°, while the beam-level beamwidth is assumed to be 30°. The total time slot duration is assumed to be $65535\mu s$, which is a combination of the alignment time and the data transmission time [13]. The pilot transmission time for beam alignment phase is considered to be $20\mu s$, where the pilot transmission time is always less than the total time slot duration.

Fig. 3 demonstrates the EE versus SE for the proposed

LDD-based scheme by dynamically tuning the priority of both the objectives resulting in the corresponding Pareto optimal solution at $\alpha = 50\%$ for various values of β. Moreover, a comparison between the proposed LDD-based scheme and the maximal-rate (maxRx), Dynamic sub-carrier allocation (DSA) [14] and Joint power and rate adaptation (JPRA) [15] algorithms is presented. In the following, we briefly explain the functionality of these schemes. The average traffic load L_{DBS} for each DBS at the 5th measuring time interval denoted by t_5, is predicted by the traffic prediction module as $L_{\text{DBS}} = [50\% \ 30\% \ 30\% \ 60\% \ 20\% \ 30\%]$, where $L_{\text{DBS}} = 50\%$ denotes 50% loading at the DBS, i.e., 5 users, as the maximum number of users assumed at the DBS=10.

- **Maximal-rate (maxRx)**
  In the first step, equal water-filling level is assumed for all users by assigning equal transmit power for all the sub-carriers. Next, the sub-carrier allocation and user association with the BSs is conducted to maximize the sum rate. The process is reduced to a single objective problem, where the achievable SE and EE for this single-objective problem at $\alpha = 50\%, \beta = [50\% \ 60\% \ 70\% \ 80\%]$ is shown in Fig. 3. MaxRx scheme provides a higher SE but a lower EE due to more power consumption as compared to the LDD-based scheme at $\alpha = 50\%, \beta = 50\%$. However, for higher values of β, both SE and EE are impacted and a lower value for both factors is observed as compared to the LDD-based scheme.

- **Dynamic sub-carrier allocation (DSA)**
  The worst sub-carriers are eliminated and equal transmit power is assumed for all the remaining sub-carriers. The sub-carrier allocation and user association is conducted to maximize the sum rate, where the scheme is based on a single objective problem. As shown in Fig. 3, DSA scheme provides a lower SE and EE as compared to the proposed LDD-based scheme.

- **Joint power and rate adaptation (JPRA)**
  The worst sub-carriers are eliminated by assigning zero power on those sub-carriers. The power of the eliminated sub-carriers is added to the total available power and is subsequently redistributed among the remaining sub-carriers. The sub-carrier allocation is fixed and the power allocation is based on the the multi-level water-filling approach for maximizing the total number of bits transmitted on each sub-carrier. It is pertinent to note that the elimination of sub-carriers reduces the network capacity, thereby leading to less SE and EE as compared to the LDD-based scheme.

Considering the results for LDD-based scheme, it can be observed that an increase in SE leads to an increase in EE up to a peak value. This trend is a result of the dominance of circuit power of the BS as compared to the transmit power. However, following the peak value, the EE decreases sharply with an increase in SE as now the transmit power dominates the total power consumption of the transmission that leads to a quasi-concave behavior of EE-SE tradeoff. The Pareto frontier curve shown in the figure also signifies three points of interest, i.e., the power minimization point, the EE maximization point,
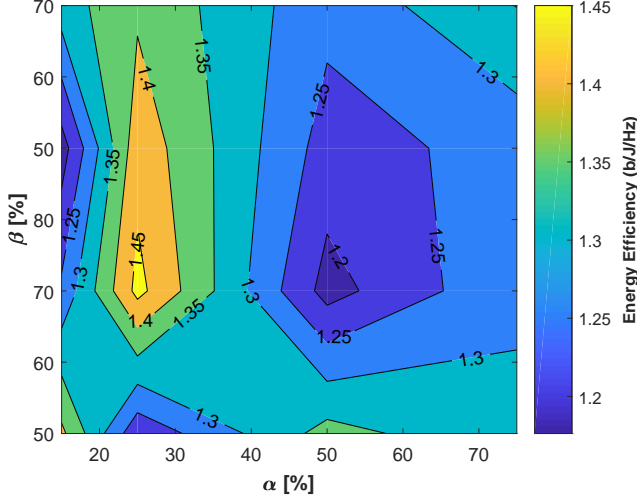
Figure 5: Energy-efficiency for the different partition sets of (α, β) at measuring time interval t_1, average traffic load $\text{L}_{\text{DBS}} = [40\% \ 25\% \ 30\% \ 45\% \ 50\% \ 35\%]$

Figure 6: Spectral-efficiency for the different partition sets of (α, β) at measuring time interval t_1, $\text{L}_{\text{DBS}} = [40\% \ 30\% \ 20\% \ 50\% \ 60\% \ 30\%]$

and the SE maximization point. These points are important from the designer's perspective, highlighting the extremities of SE/EE tradeoff.

Similarly, Fig. 4 shows the variation of EE with different partition sets of (α, β) at the 10th measuring time interval, denoted by t_{10}, where the corresponding predicted traffic load is $\text{L}_{\text{DBS}} = [40\% \ 25\% \ 30\% \ 45\% \ 50\% \ 35\%]$. This figure signifies the maximum achievable EE for the partition set (α, β), providing a designer's perspective for identifying the desired partition set. However, as discussed earlier, it is important to note that maximum achievable EE and maximum achievable SE are observed at different partition sets. For example, Fig. 4 shows that maximum EE=2.98 (b/J/Hz) can be achieved at partition set $(75\%, 50\%)$ with the corresponding SE=9.45 (b/s/Hz). On the other hand, minimum EE=1.87 (b/J/Hz) is observed at partition set $(40\%, 55\%)$, with the corresponding SE=11.5 (b/s/Hz), which signifies the impact of partition set on the EE and SE.

Fig. 5 presents the EE versus the different partition sets of (α, β) at the 1st measuring time interval denoted by t_1. The average traffic load of each DBS predicted by the traffic prediction module at t_1, is given by, $\text{L}_{\text{DBS}} = [40\% \ 30\% \ 20\% \ 50\% \ 60\% \ 30\%]$. The maximum EE of 1.45 b/J/Hz is observed for the partition set $(25\%, 60\%)$. Similarly, from Fig. 6, we can observe that the corresponding achievable SE approximately equals to 11.2 b/s/Hz for the same partition set. The 11.2 b/s/Hz observed at the same partition set $(25\%, 60\%)$ is not the maximum value of SE. It shows the corresponding SE observed at the partition set that provides maximum EE. These figures help in identifying the optimal (α, β) combination for achieving the maximum EE and the corresponding SE at that combination. If the desired criteria is to achieve maximum SE, then similar results could be obtained showing the variation of SE with (α, β) combination and the corresponding EE. The optimal combination can change with the number of users and the bandwidth available at CBS. The users leaving the network frequently could impact the
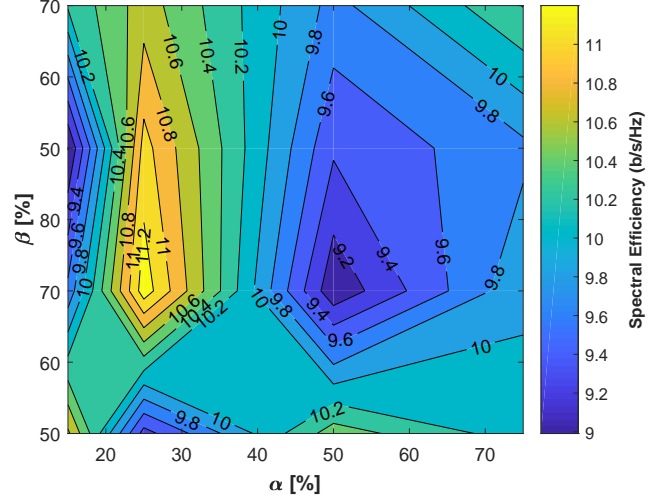
optimal combination for achieving the desired EE and SE. If several users enter the coverage area of a CBS and fall outside the coverage of all the 6 DBSs, then an optimal combination would have a higher β requirement. Similarly, an increase in the number of users lying within the coverage area of DBS but are not served by DBS would lead to a higher α requirement.

The aforementioned results depict the significance of the performance gains that can be achieved through CDSA. From a network designer's perspective, the optimal control-data partition can be identified depending on the network rate requirements and the density of the devices in the network. Moreover, the traffic load patterns influence the performance of CDSA, which signifies the need for developing new traffic prediction techniques. To summarize, the proposed network provides a direction towards employing CDSA for achieving better performance as compared to the conventional cellular networks.

IV. CONCLUSION AND FUTURE DIRECTIONS

In this article, we built the case for employing dual-band mmWave network based on CDSA, presenting a new dimension to spectrum heterogeneity. Viewing the spectrum crunch and the ever increasing demand for higher bandwidth, dual-band mmWave network could go a long way in alleviating the spectrum scarcity. The utilization of mmWave wireless communication for future 5G networks is motivated by delineating the design aspects. We reason that despite these factors, the popularity of mmWave licensed and unlicensed bands would increase with time and lead to the development of several new applications. We employ the CDSA architecture to evaluate the dual-band mmWave network by splitting the available RBs between control and data plane. A MOO problem is formulated, which jointly optimizes conflicting objectives; SE and EE. A case study is presented for analyzing the SE-EE tradeoff, providing a designer's perspective for a CDSA-based network.

As a future direction of this work, the DBS switching mechanism could be employed to analyze the network performance based on the traffic patterns. The evaluation of energy savings and the impact of switching DBS on the end-to-end transmission delay could provide significant insight into the network robustness. Although, the centralized approach followed by CDSA allows CBS/DBS coordination, the CBS needs to extract the context information such as the position of nodes for smooth coordination. The collection and storage of context information is also one of the research challenges that needs to be addressed. Moreover, the exchange of signaling information between CBS and DBS requires an ultra-reliable and low latency back-haul mechanism, which triggers the need to explore techniques that incur minimum signaling overhead for CDSA. In a nutshell, there are several aspects associated with CDSA that require further research, making them a strong contender for 5G networks.

REFERENCES

[1] Y. Liu, C. Yuen, X. Cao, N. U. Hassan, and J. Chen, "Design of a scalable hybrid mac protocol for heterogeneous m2m networks," *IEEE Internet of Things Journal*, vol. 1, no. 1, pp. 99–111, Feb 2014.

[2] R. Mahapatra, Y. Nijsure, G. Kaddoum, N. U. Hassan, and C. Yuen, "Energy efficiency tradeoff mechanism towards wireless green communication: A survey," *IEEE Communications Surveys Tutorials*, vol. 18, no. 1, pp. 686–705, Firstquarter 2016.

[3] A. M. Abdelhady, O. Amin, and M. S. Alouini, "Resource allocation for phantom cellular networks: Energy efficiency vs spectral efficiency," in *2016 IEEE International Conference on Communications (ICC)*, May 2016, pp. 1–6.

[4] K. Shen, Y. F. Liu, D. Y. Ding, and W. Yu, "Flexible multiple base station association and activation for downlink heterogeneous networks," *IEEE Signal Processing Letters*, vol. 24, no. 10, pp. 1498–1502, Oct 2017.

[5] T. Lv, Z. Lin, P. Huang, and J. Zeng, "Optimization of the energy-efficient relay-based massive iot network," *IEEE Internet of Things Journal*, vol. 5, no. 4, pp. 3043–3058, Aug 2018.

[6] S. Niknam, A. A. Nasir, H. Mehrpouyan, and B. Natarajan, "A multi-bandOFDMA heterogeneous network for millimeter wave 5G wireless applications," *IEEE Access*, vol. 4, pp. 5640–5648, 2016.

[7] J. Deng, O. Tirkkonen, R. Freij-Hollanti, T. Chen, and N. Nikaein, "Resource allocation and interference management for opportunistic relaying in integrated mmwave/sub-6 GHz 5G networks," *IEEE Communications Magazine*, vol. 55, no. 6, pp. 94–101, 2017.

[8] A. Mohamed, O. Onireti, M. A. Imran, A. Imran, and R. Tafazolli, "Control-data separation architecture for cellular radio access networks: A survey and outlook," *IEEE Communications Surveys Tutorials*, vol. 18, no. 1, pp. 446–465, Firstquarter 2016.

[9] C. Yang, J. Li, Q. Ni, A. Anpalagan, and M. Guizani, "Interference-aware energy efficiency maximization in 5g ultra-dense networks," *IEEE Transactions on Communications*, vol. 65, no. 2, pp. 728–739, Feb 2017.

[10] Z. Li, S. Gong, C. Xing, Z. Fei, and X. Yan, "Multi-objective optimization for distributed mimo networks," *IEEE Transactions on Communications*, vol. 65, no. 10, pp. 4247–4259, Oct 2017.

[11] T. Bai and R. W. Heath, "Coverage and rate analysis for millimeter-wave cellular networks," *IEEE Transactions on Wireless Communications*, vol. 14, no. 2, pp. 1100–1114, Feb 2015.

[12] E. Turgut and M. C. Gursoy, "Coverage in heterogeneous downlink millimeter wave cellular networks," *IEEE Transactions on Communications*, vol. 65, no. 10, pp. 4463–4477, Oct 2017.

[13] H. Shokri-Ghadikolaei, L. Gkatzikis, and C. Fischione, "Beam-searching and transmission scheduling in millimeter wave communications," in *2015 IEEE International Conference on Communications (ICC)*, June 2015, pp. 1292–1297.

[14] D. S. W. Hui, V. K. N. Lau, and W. H. Lam, "Cross-layer design for ofdma wireless systems with heterogeneous delay requirements," *IEEE Transactions on Wireless Communications*, vol. 6, no. 8, pp. 2872–2880, August 2007.

[15] S. Singh, M. Shahbazi, K. Pelechrinis, K. Sundaresan, S. V. Krishnamurthy, and S. Addepalli, "Adaptive sub-carrier level power allocation in ofdma networks," *IEEE Transactions on Mobile Computing*, vol. 14, no. 1, pp. 28–41, Jan 2015.